New Framework for Optimal Current Sharing of non-identical Parallel Buck Converters Extended version

Romain Delpoux, Jean-François Trégouët, Jean-Yves Gauthier, Cyril Lacombe

New Framework for Optimal Current Sharing of non-identical Parallel Buck Converters Extended version

Romain Delpoux, Jean-François Trégouët, Jean-Yves Gauthier and Cyril Lacombe
Laboratoire Ampère CNRS UMR 5005, Université de Lyon, INSA - Lyon,
25 avenue Jean Capelle, 69621 Villeurbanne, France
Email: romain.delpoux@insa-lyon.fr

This report is an extended version of the corresponding submission to TCST which does not included blue parts of this document.

***Abstract*—In this paper, parallel interconnection of buck (step-down) converters is considered. Classical control of such a topology uniformly distributes load current over branches. Yet, whenever non-identical converters (having distinct characteristics) are considered, this paper demonstrates, both theoretically and experimentally, that minimizing overall losses requires non uniform and even load-depend current distribution. In this context, a novel highly modular hierarchical control framework is proposed for arbitrary number of buck converters. Solutions for the two related design steps are given, which leads to a control law minimizing total losses as well as correcting voltage deviation for any operating point and without knowledge about load magnitude. Several formal statements and experimental results support our discussions.**

I. Introduction

Substituting a single high-capacity centralized electrical power converter by multiple distributed converters connected in parallel is a strategy that becomes more and more popular. Indeed, paralleling converters offers several advantages such as increased reliability due to redundancy and distribution of stresses of components [1], ease of maintenance and repair, improved thermal management [2] and reduced output ripple by interleaving phase of Pulse Width Modulation (PWM) [3].

An essential feature offered by parallel interconnection of converters is the possibility to distribute load current. Indeed, if regulation of output voltage imposes overall current, distribution of current among converters remains free. The most wide-spread strategy for dealing with this degree of freedom is the so-called balanced current sharing which uniformly distributes currents among converters [3], [1], [2]. Whenever identical converters (same class of converters sharing the same electrical components) are considered, this policy is fully justified by the fact that it equally distributes stresses among converters as well as minimizes overall losses. However, few papers in the literature consider interconnection of non-identical converters for which balanced current sharing is expected not to be the optimal.

To the best of the authors' knowledge, existing solutions to achieve nonuniform current sharing relies on "virtual droop resistors" which can be interpreted as a low-frequency negative feedback (the feedback gain is the so-called "droop resistor") on current which aims adjusting equilibrium current [4], [5]. Then a rule of thumb is to fix the droop resistor magnitude for bus voltage to remain into allowed bounds when the converter injects its maximum power [6], [4]. As noticed in [5], this strategy maintains constant current ratio between converters, whereas optimal current sharing requires load dependent current ratio, as formally demonstrated in this paper.

1) Our first contribution is to provide a rigorous statement of the control problem related to parallel interconnection of arbitrary number of non-identical (having distinct characteristics) buck DC/DC converters with the requirement of converging to the optimal steady-state with respect to power losses. Corresponding electrical circuit is depicted by Fig. 1. This treatment proves, both theoretically and experimentally, not only that balanced current sharing cannot be optimal for all load with respect to overall power losses but also that optimal current ratio is in general load-dependent (Section IV). 2) As a second contribution, a sequential design procedure leading

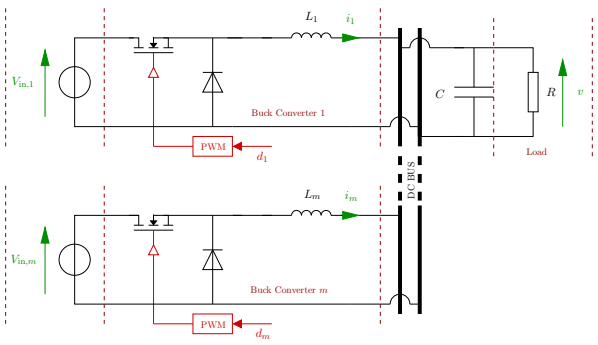

Fig. 1. Electrical schematic.

to two control layers evolving at different time-scales is proposed as a suitable framework for solving the underlying control problem, without knowledge about load magnitude. Rigorous formalization of requirements and assumptions of each step is provided (Section V). 3) Building on this statement, our third and main contribution implements this procedure and gives rise to (i) a stabilizing fast time-scale inner controller (Section VI) working in concert with (ii) an outer controller canceling voltage deviation as well as imposing optimal current distribution for all load (Section VII). Then, extensive experimental results for the full control scheme validate discussions of this paper (Section VIII).

A preliminary version of this paper was presented in [7]. Here, as compared to [7], we illustrate modularity of the proposed framework by deriving a new outer controller which is demonstrated to be compatible with any stabilizing inner controller satisfying mild assumptions, we provide several statements and proofs of the stability properties of the proposed schemes, and we provide real experimental validation relying on inner controller benefiting from higher robustness properties than that of [7].

Notation: The symbol $\mathbf{I}_m$ stands for the identity matrix of dimensions $m \times m$. The null matrix of size $m \times n$ is denoted by $\mathbf{0}_{m\times n}$. The vector (column matrix) of size m for which every entry is 1 is denoted by $\mathbf{1}_m$. The notation x_k refers to the k-th element of the vector x, with 1 being the index of the first element. The operator 'diag' builds diagonal matrix from entries of the input vector argument. The steady-state value of the signal $\zeta(t)$ is denoted by $\zeta^\star$, i.e. $\zeta^\star = \lim_{t\to+\infty} \zeta(t)$.

II. Problem statement

The electrical circuit represented by Fig. 1 is considered. It mimics the parallel interconnection of m buck converters that would share a single capacitor.

Converters are controlled via PWM and d_k refers to duty cycle of k-th converter. The control aims regulating DC bus voltage v to desired level V_{ref}, i.e.

$$v^\star = V_{\text{ref}}, \tag{1}$$

where $v^\star$ refers to the asymptotic value of $v(t)$, for any positive and *unknown* load R. Imposing (1) is equivalent to saying that the sum $i_T^\star$ of each $i_k^\star$ is equal to V_{ref}/R, where i_k referd to current in k-th inductors L_k. Thus, additional degrees of freedom remain in the way $i_T^\star$ is distributed among converters. For this reason, this paper introduces minimization of the steady-state global losses as an additional requirement for the outer controller. Note that losses due to parasitic elements of capacitor C depends on $i_T^\star$ exclusively, which makes it completely independent from current sharing policy. Hence, the quantity to be minimized is $p_T^\star$ defined as

$$p_T(i) := \textstyle\sum_{k\in\mathcal{K}} p_k(i_k) \quad \text{with} \quad \mathcal{K} := \{1, \cdots, m\}, \tag{2}$$

where p_k refers to power losses due to MOSFET, diode and inductor of k-th converter.

III. Model description

Power losses are considered by taking parasitic elements of electrical components of Fig. 1 into account. Following the methodology proposed by [8, Sec. 2.2.11] for a single buck converter, the equivalent circuit depicted by Fig. 2 is derived from Fig. 1. For the k-th converter, $R_{S,k}$ is the MOSFET on-resistance, $R_{F,k}$ is the diode forward resistance, $V_{F,k}$ is the diode threshold voltage and $R_{L,k}$ is the equivalent series resistance (ESR) of the inductor L_k. Resistance R_C refers to the ESR of the filter capacitor C.

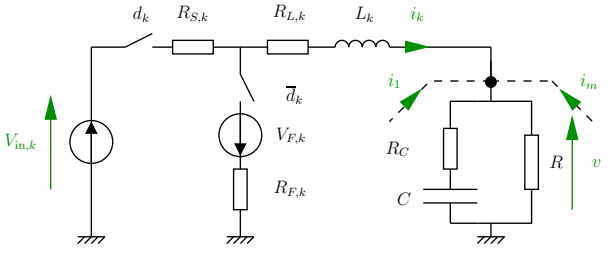

Fig. 2. Equivalent circuit of Fig. 1 with parasitic resistances and the diode offset voltage.

Throughout this paper, it is assumed that (i) frequency of the commutation f_s is sufficiently large for the dynamics to be approximated by an average (ripple-free) continuous-time model and (ii) converters operate in continuous conduction mode. In addition to that, the following hypothesis is made.

Assumption 1. For each converter, magnitudes of the MOSFET on-resistance and the diode forward resistance are equal, i.e. $R_{F,k} = R_{S,k}, (k \in \mathcal{K})$. △

By virtue of Kirchhoff's circuit laws, under previous assumptions, dynamics of the circuit is governed by

$$\begin{aligned} \forall k \in \mathcal{K},\ L_k \frac{di_k}{dt} &= -v - (R_{L,k} + R_{F,k}) i_k \\ &\quad + (V_{\text{in},k} + V_{F,k}) d_k - V_{F,k}, \qquad (3a) \\ C(R + R_C)\frac{dv}{dt} - CRR_C \frac{di_T}{dt} &= Ri_T - v, \qquad (3b) \end{aligned}$$

where

$$i_T := \textstyle\sum_{k\in\mathcal{K}} i_k = \mathbf{1}_m^\intercal\, i, \qquad (3c)$$

refers to the total current. From [8, Eq. (2.134)] and [9], average power losses p_k is given by

$$\begin{aligned} p_k &= (R_{F,k} + R_{L,k}) i_k^2 - V_{F,k} i_k d_k \\ &\quad + (V_{F,k} + t_{\text{SW},k} f_s V_{\text{in},k}) i_k, \qquad (4) \end{aligned}$$

where inductor losses are described by $R_{L,k} i_k^2$, conduction losses by $R_{F,k} i_k^2 + V_{F,k}(1 - d_k) i_k$ and commutation losses are approximated by $t_{\text{SW},k} f_s V_{\text{in},k} i_k$, $t_{\text{SW},k}$ being related to switching shape and duration.

Remark (Hypothesis on $R_{S,k}$ and $R_{F,k}$). Without Assumption 1, additional terms multiplied by $(R_{S,k} - R_{F,k})$ have to be introduced in both (3a) and (4). Nevertheless, such a hypothesis is fully justified by the fact that magnitude of $R_{S,k}$ and $R_{F,k}$ are of the same order and smaller than $R_{L,k}$, allowing those terms to be neglected. Experimental results provided by Section VIII-A validate this statement. Note that fine stability analysis could be performed by means of standard robust analysis tools treating those terms as a small state-dependent perturbation (see e.g. [10]). ⌟

IV. Optimal current distribution

Equating derivatives of v and i_k to zero in (3) gives

$$\begin{aligned} \forall k \in \mathcal{K},\ i_k &= \frac{-(V_{\text{in},k} + V_{F,k}) d_k + V_{F,k} + v}{-R_{L,k} - R_{F,k}}, \qquad (5) \\ v &= Ri_T. \qquad (6) \end{aligned}$$

which characterizes the set of all possible equilibria, among which $(i_{\text{opt}}, V_{\text{ref}})$ is of particular interest as it minimizes p_T for $v = V_{\text{ref}}$, i.e.

$$i_{\text{opt}}(R) := \arg\min_{i^\star} p_T(i^\star) \quad \text{s.t.} \quad (1). \qquad (7)$$

In order to derive expression of i_{opt}, let us rewrite d_k in terms of i_k and v via (5) and substitute this expression in (4) for $v = V_{\text{ref}}$. This gives

$$p_k = r_{1,k} i_k^2 + r_{2,k} i_k, \qquad (8)$$

with

$$\begin{aligned} r_{1,k} &= V_{\text{in},k}(R_{F,k} + R_{L,k})/(V_{\text{in},k} + V_{F,k}), \\ r_{2,k} &= -V_{F,k}(V_{F,k} + V_{\text{ref}})/(V_{\text{in},k} + V_{F,k}) \\ &\quad + V_{F,k} + f_s t_{\text{SW},k} V_{\text{in},k}. \end{aligned}$$

As a result, i_{opt} minimizes quadratic cost function (8) under linear constraint $R\mathbf{1}_m^\intercal i_{\text{opt}} = V_{\text{ref}}$ corresponding to (6) and, in turn, admits an analytical expression.

Proposition IV.1. *Current vector i_{opt}, defined by (7) reads*

$$i_{\text{opt}}(R) = (\mathbf{1}_m - \Gamma\Psi r_1)\, V_{\text{ref}}/(mR) - \Gamma\Psi r_2/2, \qquad (9)$$

where $\Psi \in \mathbb{R}^{(m-1)\times m}$ and $\Gamma \in \mathbb{R}^{m\times(m-1)}$ refer to

$$\begin{aligned} \Psi &:= (\Gamma^\intercal \text{diag}\{r_1\}\,\Gamma)^{-1}\Gamma^\intercal, \qquad (10) \\ \Gamma &:= \begin{bmatrix} \mathbf{I}_{m-1} \\ \mathbf{0}_{1\times m-1} \end{bmatrix} - \begin{bmatrix} \mathbf{0}_{1\times m-1} \\ \mathbf{I}_{m-1} \end{bmatrix}. \qquad (11) \end{aligned}$$

Proof. The set of solutions of (1) can be parametrized by $q \in \mathbb{R}^{m-1}$ as follows

$$i(q) = V_{\text{ref}}/(Rm)\mathbf{1}_m + \Gamma q, \qquad (12)$$

since columns of Γ form a basis of $\text{Ker}\,\{\mathbf{1}_m^\intercal\}$. Rewriting $p_T(i)$ as

$$p_T = i^\intercal \text{diag}\{r_1\}\, i + r_2^\intercal i, \qquad (13)$$

allows to compute the derivative $\partial p_T(i(q))/\partial q$ which is equal to zero if and only if

$$q = -(\Gamma^\intercal \text{diag}\{r_1\}\,\Gamma)^{-1}\Gamma^\intercal (V_{\text{ref}}/(Rm) r_1 + r_2/2),$$

since Γ is full column rank. Substituting the previous expression of q in (12) gives (9). □

Let us now illustrates this result for the experimental setup conditions described in Section VIII for two converters ($m = 2$). Fig. 3 depicts power loss levels $p_T(i_1, i_2)$ (2) with identified parameters $r_{1,2}$ (colored elliptical sections), as well as the algebraic relation (6) for $v = V_{\text{ref}}$ (black segment), reading $i_1 + i_2 = V_{\text{ref}}/R$. The dashed blue line represents

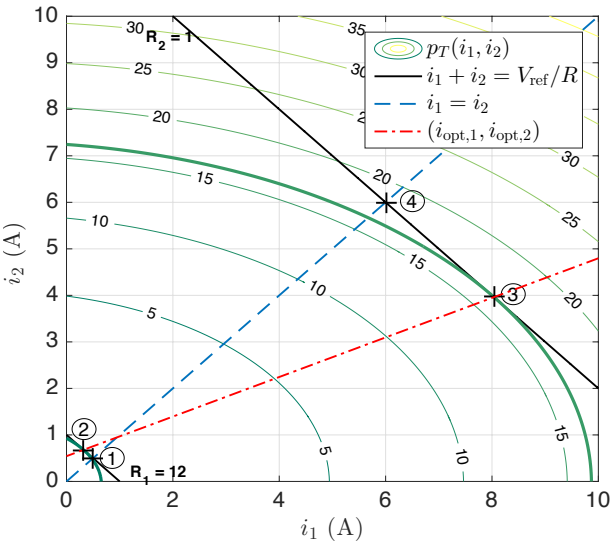

Fig. 3. Power levels and optimal currents.

uniform current distribution $i_1 = i_2$. The location of optimal losses in the converters as function of the load is represented by the dashed red line, issued from (9). Note that this line is straight as $i_{\rm opt}$ is affine with respect to $1/R$.

As these two lines do not overlap, uniform current distribution cannot be optimal for all R. Nonetheless, this is the case for the specific load value for which the lines intersect. For lower output power corresponding to higher load magnitude, $i_{\rm opt,2}$ exceeds $i_{\rm opt,1}$ so that most of the power should be convey by converter 2, whereas the opposite ordering should to be preferred for higher output power. Such an observation is made possible by the fact that the dashed red line is only affine (and not linear) so that lines intersect and, in turn, $i_{\rm opt,1}$ is not a constant (that is, load independent) fraction of $i_{\rm opt,2}$, i.e. optimal current ratio depends on R. The fact that inequalities $r_{1,1} < r_{1,2}$ and $r_{2,1} > r_{2,2}$ hold in this case is the reason behind this optimal current inversion: At low load current, where $r_{2,k} i_k$ dominates $r_{1,k} i_k^2$ in expression of p_k given by (8), the use of converter 2 is preferable whereas priority should be given to converter 1 at high load current, where ordering of the two terms of p_k is reversed. Section VIII relates this observation to the electrical characteristics of the converters.

Remark (Load dependent current ratio). Let us illustrate load dependency of converter ratings in the case of two converters ($m = 2$). In such a case, (9) reads

$$i_{\rm opt} = \begin{bmatrix} \dfrac{r_{1,2}}{r_{1,1}+r_{1,2}} \\ \dfrac{r_{1,1}}{r_{1,1}+r_{1,2}} \end{bmatrix} \frac{V_{\rm ref}}{R} - \begin{bmatrix} \dfrac{r_{2,1}-r_{2,2}}{2(r_{1,1}+r_{1,2})} \\ \dfrac{r_{2,2}-r_{2,1}}{2(r_{1,1}+r_{1,2})} \end{bmatrix},$$

so that ratio $i_{\rm opt,1}/i_{\rm opt,2}$ is a function of R:

$$\frac{i_{\rm opt,1}}{i_{\rm opt,2}} = \frac{2V_{\rm ref} r_{1,2} - R(r_{2,1}-r_{2,2})}{2V_{\rm ref} r_{1,1} - R(r_{2,2}-r_{2,1})}.$$

Note that independency with respect to R is recovered whenever $\Gamma \Psi r_2/2 = \mathbf{0}$, so that $i_{\rm opt}$ admits a linear expression with respect to $1/R$. This happens if terms $r_{2,k}$ are identical for all k which implies that $r_2 = \mathbf{1}_m r_{2,1}$ and, in turn, leads to $\Psi r_2 = \mathbf{0}$ since $\Gamma^\intercal \mathbf{1}_m = \mathbf{0}$. ⌟

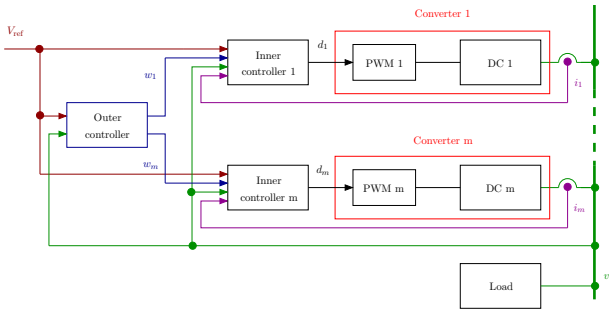

Fig. 4. Considered control hierarchy.

V. New hierarchical control framework

In order to solve the aforementioned problem, a control framework relying on two nested control loops is proposed in this section.

On the first hand, local *inner controllers* ensure stability of the overall system as well as droop control[1] for all resistive load by relying only on local information: v and i_k. On the other hand, centralized *outer controller* communicates with every inner controllers by delivering a signal w_k in order to drive the overall system to the optimal steady-state by relying on measurement of v exclusively. Typically, w_k adjusts voltage reference viewed by individual k-th inner controller to $V_{\rm ref} + w_k$ instead of $V_{\rm ref}$.

Step 1 (Inner loop design)**.** Find a load-independent controller $d(i_k, v, w_k)$ such that induced dynamics of i and v asymptotically converge to some equilibrium $i_e(w, R)$ and $v_e(w, R)$ for all constant signal $w \in \mathbb{R}^m$

[1]In this context, droop control refers to a proportional negative feedback on current (see [6, eq. (17)]).

and for all constant load $R \in \mathbb{R}_{>0}$. Besides, voltage equilibrium v_e depends on every w_k. •

The last sentence of Step 1 can be interpreted as a controllability requirement for the design of the outer controller. Indeed, this control layer will be able to impose a particular current distribution only if w_k impacts i_k for all k. This is indeed the case if voltage equilibrium $v_e = Ri_T$ is a function of every w_k. This means that signals w_k cannot be rejected by inner controller as a perturbation. Consequently, any integral action on voltage v aiming at regulating asymptotic value of v to V_{ref} (regardless of w_k) is prohibited at the inner control layer.

Remark (Inner control design). The distributed control problem underlying the design of linear inner control can be formulated as follows: Find the stabilizing state feedback $d = d_0 + K(s)x$ where $x = (i, v)$ and $K(s)$ is a (possibly dynamic) sparse matrix of the form

$$K(s) = \begin{bmatrix} \star & 0 & \cdots & 0 & \star \\ 0 & \star & \ddots & \vdots & \star \\ \vdots & \ddots & \ddots & 0 & \vdots \\ 0 & \cdots & 0 & \star & \star \end{bmatrix} \in \mathbb{R}^{m\times(m+1)}, \quad (14)$$

where $\star$ denotes non-zero entry. ⌟

Step 2 (Outer loop design). Given an inner controller solving Step 1, find an outer control law $w(v)$ imposing the steady-state characterized by (1) and $i^\star = i_{\text{opt}}(R)$ for all load $R \in \mathbb{R}_{>0}$. •

It is emphasis that load is *not measured* so that neither inner nor outer controller can depend on R. In addition to that, particular care should be taken to prevent nested loops to badly interacts.

Remark (Communications between control layer). It is worth mentioning that communication from outer to inner controllers is unidirectional – i_k is not required for w_k to be computed – and low bandwidth – dynamics induced by this outer control is slower than that of the inner control – which has obvious implementation advantages in the case where converters are distant. In the same vein, observe that if w_k is used by the inner controllers, this signal is not required to guarantee stability which is ensured even if $w_k \equiv 0$, resulting for instance when communication network brakes down. ⌟

VI. Inner controller design

In this section, a class of satisfying local inner controller is first proposed. It can be regarded as sufficient conditions for Step 1 to be satisfied. This control law reads as follows

$$d_k = \left(\alpha_k(V_{\text{ref}} + w_k) - (\alpha_k - 1)v - \beta_k i_k\right)/V_{\text{in},k}, \quad (15)$$

and has two real parameters, α_k and β_k. Being added to V_{ref}, observe that the output w_k of the outer controller can be interpreted as a voltage reference shift from the inner control view point.

Introducing $\alpha'_k := (\alpha_k - 1)/\kappa_k + 1$, $\kappa_k := V_{\text{in},k}/(V_{\text{in},k} + V_{F,k})$ and $v_C := v - R_C(i_T - v/R)$ which can be physically interpreted as the voltage of capacitor C, asymptotic stability of $x_c := [i\ v_C]^\intercal$ and, in turn, v can be established via Lyapunov function $V(x_c) := x_c^\intercal P x_C$, with

$$P := \text{diag}\{L_1/\alpha'_1, \ldots, L_m/\alpha'_m, C\}/2,$$

for any $R > 0$, and α_k and β_k sufficiently large. In such a case, it happens that voltage equilibrium v_e must depend on each w_k.

Proposition VI.1 (Sufficient condition). *For any $\alpha_k > V_{F,k}/(V_{\text{in},k} + V_{F,k})$ and $\beta_k > -(R_{L,k} + R_{F,k})V_{\text{in},k}/(V_{\text{in},k} + V_{F,k})$, ($k \in \mathcal{K}$), inner controller (15) solves Step 1.*

Proof. First observe that law (15) modifies (3a) as follows

$$\begin{aligned} L_k\frac{di_k}{dt} &= -\alpha'_k(v - V_{\text{ref}} - w_k) - \beta'_k i_k \\ &\quad +(1/\kappa_k - 1)(V_{\text{ref}} + w_k) - V_{F,k}, \end{aligned} \quad (16)$$

where $\beta'_k := \beta_k/\kappa_k + R_{L,k} + R_{F,k}$. Then, from the definition of v_C, it comes out that

$$v = R_{\text{eq}}/R_C v_C + R_{\text{eq}} i_T \quad (17)$$

with $R_{\text{eq}} := RR_C/(R + R_C)$. Substitution of this expression into (3b) and (16) gives

$$\begin{aligned} L_k\frac{di_k}{dt} &= -\frac{\alpha'_k R_{\text{eq}}}{R_C}v_C + \alpha'_k(V_{\text{ref}} + w_k) - \beta'_k i_k \\ &\quad -\alpha'_k R_{\text{eq}} i_T + (1/\kappa_k - 1)(V_{\text{ref}} + w_k) - V_{F,k} \\ C\frac{dv_C}{dt} &= \frac{R_{\text{eq}}}{R_C}i_T - \frac{1}{R + R_C}v_C \end{aligned}$$

or, equivalently,

$$\begin{aligned} \frac{d}{dt}\begin{bmatrix} i \\ v_C \end{bmatrix} &= A_C \begin{bmatrix} i \\ v_C \end{bmatrix} + B_C(V_{\text{ref}}\mathbf{1}_m + w) \\ &\quad - \begin{bmatrix} \text{diag}\{L\}^{-1}V_F \\ 0 \end{bmatrix} \end{aligned} \quad (18)$$

with

$$A_C := \text{diag}\left\{\begin{bmatrix} L \\ C \end{bmatrix}\right\}^{-1} \begin{bmatrix} M & -R_{\text{eq}}/R_C\alpha' \\ R_{\text{eq}}/R_C\mathbf{1}_m^\intercal & -1/(R + R_C) \end{bmatrix}$$

$$B_C := \begin{bmatrix} \mathrm{diag}\{L\}^{-1}\,\mathrm{diag}\{\nu\}\,\mathrm{diag}\{\beta'\} \\ \mathbf{0}_{1\times m} \end{bmatrix}$$

$$M := -\mathrm{diag}\{\beta'\} - R_{\mathrm{eq}}\mathrm{diag}\{\alpha'\}\,\mathbf{1}_m\mathbf{1}_m^\intercal$$

and where ν_k is given by

$$\nu_k := (\alpha'_k + 1/\kappa_k - 1)/\beta'_k \in \mathbb{R}. \tag{19}$$

To prove that A_C is Hurwitz, first observe that

$$\alpha'_k > 0,\ \beta'_k > 0,\ (k \in \mathcal{K})$$

hold for any α and β selected as in the statement of Proposition VI.1. As a result, Lyapunov function $V(x_c)$ is positive definite which ensures that $A_C^\intercal P + PA_C$ given by

$$\begin{bmatrix} \mathrm{diag}\{\alpha'\}^{-1} M & \mathbf{0}_{m\times 1} \\ \mathbf{0}_{1\times m} & -\dfrac{1}{R+R_C} \end{bmatrix}$$

is negative definite since

$$\mathrm{diag}\{\alpha'\}^{-1} M = -\mathrm{diag}\left\{\frac{\beta'_1}{\alpha'_1},\ldots,\frac{\beta'_m}{\alpha'_m}\right\} - R_{\mathrm{eq}}\mathbf{1}_m\mathbf{1}_m^\intercal$$

is negative definite for all $R > 0$. This proves that dynamics of i and v_C are asymptotically stable. As $R > 0$, asymptotically stability of v is also guarantied.

Let us now prove that voltage equilibrium v_e depends on each w_k. To this end, observe that

$$\begin{aligned} v_e &= R_{\mathrm{eq}}\begin{bmatrix}\mathbf{1}_m^\intercal & 1/R_C\end{bmatrix}\begin{bmatrix} i \\ v_c\end{bmatrix} \\ &= -R_{\mathrm{eq}}\begin{bmatrix}\mathbf{1}_m^\intercal & 1/R_C\end{bmatrix} \\ &\quad A_C^{-1}\left(B_C(V_{\mathrm{ref}}\mathbf{1}_m + w) - \begin{bmatrix}\mathrm{diag}\{L\}^{-1}V_F \\ 0\end{bmatrix}\right) \end{aligned}$$

can be derived from (17) and (18) (recall that A_C is Hurwitz and, hence, invertible). Assume, by contradiction, that there exists $k_0 \in \mathcal{K}$ such that v_e does not depend on w_{k_0}. As $R_{\mathrm{eq}} \neq 0$ for all $R > 0$, this implies that

$$\begin{bmatrix}\mathbf{1}_m^\intercal & 1/R_C\end{bmatrix} A_C^{-1} B_C e_{k_0} = 0$$

where e_k is the k-th unit vector. This induces that there exists a non-zero vector $\eta \in \mathbb{R}^m$ satisfying

$$A_C^{-1} B_C e_{k_0} = \begin{bmatrix}\Gamma & \mathbf{1}_m \\ \mathbf{0} & -mR_C\end{bmatrix}\eta \tag{20}$$

since

$$\mathrm{Ker}\left\{\begin{bmatrix}\mathbf{1}_m^\intercal & 1/R_C\end{bmatrix}\right\} = \mathrm{Im}\left\{\begin{bmatrix}\Gamma & \mathbf{1}_m \\ \mathbf{0} & -mR_C\end{bmatrix}\right\}.$$

From the expression of A_C, it comes out that

$$\begin{aligned} &A_C\begin{bmatrix}\Gamma & \mathbf{1}_m \\ \mathbf{0} & -mR_C\end{bmatrix} = \\ &-\mathrm{diag}\left\{\begin{bmatrix}L \\ C\end{bmatrix}\right\}^{-1}\mathrm{diag}\left\{\begin{bmatrix}\beta' \\ 1\end{bmatrix}\right\}\begin{bmatrix}\Gamma & \mathbf{1}_m \\ \mathbf{0} & -m\end{bmatrix} \end{aligned}$$

so that

$$\begin{bmatrix}-\nu_{k_0}e_{k_0} \\ 0\end{bmatrix} = \begin{bmatrix}\Gamma & \mathbf{1}_m \\ \mathbf{0} & -m\end{bmatrix}\eta \tag{21}$$

holds from (20) and the definition of B_C. Remarking that

$$\begin{bmatrix}\Gamma & \mathbf{1}_m\end{bmatrix}^{-1} = \begin{bmatrix}(\Gamma^\intercal\Gamma)^{-1}\Gamma^\intercal \\ 1/m\mathbf{1}_m^\intercal\end{bmatrix},$$

the first m lines of (21) implies

$$-\nu_{k_0}\begin{bmatrix}(\Gamma^\intercal\Gamma)^{-1}\Gamma^\intercal \\ 1/m\mathbf{1}_m^\intercal\end{bmatrix}e_{k_0} = \eta$$

so that $\eta_m = -\nu_{k_0}/m\mathbf{1}_m^\intercal e_{k_0} = -\nu_{k_0}/m$, whereas the last $m+1$ line of (21) requires that $\eta_m = 0$. This is a contradiction since $G = \mathrm{diag}\{\nu\}$ is an invertible matrix by virtue of Lemma VI.2. This proves that v_e depends on each w_k. □

Remark (Comparison with [7]). In contrast with inner control law proposed in [7], controller (15) does not depend on system parameters (but $V_{\mathrm{in},k}$, which is assumed to be measurable), which has obvious robustness advantages. Also, closed-loop stability conditions stated by Proposition VI.1 are easily met since $V_{F,k}$, $R_{L,k}$ and $R_{F,k}$ are typically of small magnitudes so that lower bounds of α_k and β_k are slightly positive and negative, respectively. ⌟

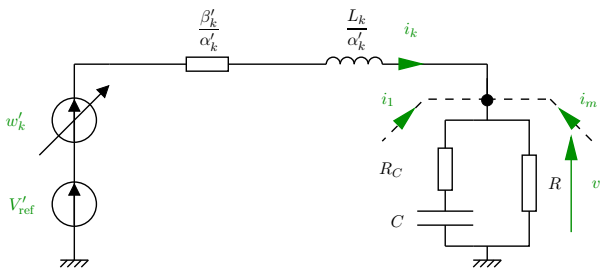

Fig. 5. Equivalent circuit to dynamics of the closed-loop system with primary control.

Remark (Selection of α_k and β_k). Relationship (16) allows to interpret α'_k and β'_k as virtual electrical stiffness and damping associated to the k-th branch, respectively. This gives a way to adjust α_k and β_k within the range defined by Proposition VI.1. To this end, another approach relies on Kirchhoff's circuit

laws which gives a way to physically interpret closed-loop equations (3b), (3c) and (16) as the dynamics induced by virtual electrical circuit depicted by Fig. 5 by rewriting (16) as

$$\frac{L_k}{\alpha'_k}\frac{di_k}{dt} + \frac{\beta'_k}{\alpha'_k} i_k = V'_{\mathrm{ref},k}(\alpha'_k) + w'_k(\alpha'_k) - v,$$

where $V'_{\mathrm{ref},k}(\alpha'_k) := V_{\mathrm{ref}} - (V_{F,k}/\alpha'_k)(V_{\mathrm{in},k} - V_{\mathrm{ref}})/V_{\mathrm{in},k}$ and $w'_k(\alpha'_k) := w_k(V_{F,k}/(\alpha'_k V_{\mathrm{in},k}) + 1)$. Comparing to Fig. 2, for every converter k, the pair MOSFET and diode is replaced by constant voltage source $V'_{\mathrm{ref},k}$ in series with a controllable voltage source w'_k. Note that $V'_{\mathrm{ref},k}(\alpha'_k) \approx V_{\mathrm{ref}}$ and $w'_k(\alpha'_k) \approx w_k$ when $V_{F,k}/\alpha'_k$ is of small magnitude. Also, the inductor value becomes L_k/α'_k with an ESR equal to β'_k/α'_k. This observation can serve as guidelines for the selection of parameters α_k and β_k. Transient duration associated with each converter can be assigned via β'_k (and, in turn, β_k) since time constant associated with k-th inductor corresponds to $(L_k/\alpha'_k)/(\beta'_k/\alpha'_k) = L_k/\beta'_k$. Additionally, α_k can be used to control (via α'_k) the steady-state when outer controller is disconnected since $i^\star_k|_{w_k=0} = \alpha'_k(V'_{\mathrm{ref},k}(\alpha'_k) - v^\star)/\beta'_k$. ⌟

Remark (Comparison with [6]). The inner controller proposed by [6, Fig. 23] adopts a two-stage form where a current inner loop delivers the duty cycle via

$$d_k = \tau_{i,k}(s)(i_{\mathrm{ref},k} - i_k),$$

from the ouput $i_{\mathrm{ref},k}$ of a voltage outer loop reading

$$i_{\mathrm{ref},k} = \tau_{\mathrm{ref},k}(s)(V_{\mathrm{ref}} + w_k - R_{D,k} i_k) + \tau_{v,k}(s) v,$$

so that the overall control law can be written as

$$\begin{aligned} d_k &= \tau_{i,k}(s)\tau_{\mathrm{ref},k}(s)(V_{\mathrm{ref}} + w_k) + \tau_{i,k}(s)\tau_{v,k}(s) v \\ &\quad -\tau_{i,k}(s)(1 + \tau_{\mathrm{ref},k}(s) R_{D,k}) i_k, \end{aligned}$$

which parameters are transfer functions $\tau_{i,k}$, $\tau_{\mathrm{ref},k}$ and $\tau_{v,k}$. By selecting those transfer functions as static gains equals to $\beta/V_{\mathrm{in},k}$, α_k/β_k, and $(1-\alpha_k)/\beta_k$, respectively, and setting $R_{D,k} = 0$, this formulation boils down to our control law (15).[2] Consequently, as compared to [6], this paper provides formal closed-loop stability certificate for a particular version of control law considered in [6]. ⌟

Let us now anticipate the outer loop design which aims driving inner closed-loop equilibrium to the optimal steady-state. Indeed, for this problem to be solved, some knowledge about how inner closed-loop behaves is required. Focusing on the steady-state, next lemma gives an answer to this question, which can be interpreted as a necessary condition for Step 1 to be solved.

Assumption 2. Inner controller is linear, time-invariant, proper and continuous. △

Lemma VI.2 (Necessary condition)**.** *For any inner controller satisfying Assumption 2 and solving Step 1, there exist load-independent $N \in \mathbb{R}^m$, $i_0 \in \mathbb{R}^m$ and $G \in \mathbb{R}^{m\times m}$ such that the stable equilibrium point (i, v) satisfies*

$$i = Gw - Nv + i_0. \tag{22}$$

Furthermore, N satisfies the following inequality

$$\mathbf{1}_m^\intercal N \geq 0, \tag{23}$$

and G is an invertible diagonal matrix.

Proof. Any inner control law completing Step 1 can be parametrized by load-independent proper transfer functions $d_{i,k}(s)$, $d_{v,k}(s)$, $d_{w,k}(s)$ and constant scalar $d_{0,k}$ as follows

$$\begin{aligned} d_k(s) &= d_{i,k}(s) i_k(s) + d_{v,k}(s) v(s) + d_{w,k}(s) w_k/s \\ &\quad + d_{0,k}/s. \end{aligned}$$

as w is supposed to be constant. Substituting $d_k(s)$ by this expression in Laplace transform of (3a) gives

$$\begin{aligned} h_k(s) i_k(s) &= ((V_{\mathrm{in},k} + V_{F,k}) d_{v,k}(s) - 1) v(s) - V_{F,k}/s \\ &\quad + (V_{\mathrm{in},k} + V_{F,k}) d_{0,k}/s + (V_{\mathrm{in},k} + V_{F,k}) d_{w,k}(s) w_k/s, \end{aligned}$$

where $h_k(s) := R_{L,k} + R_{F,k} + L_k s - (V_{\mathrm{in},k} + V_{F,k}) d_{i,k}(s)$. Since $h_k(s)$ is not identically zero for all proper function $d_{i,k}(s)$, this leads to a relationship of the form

$$i(s) = G(s) w/s - N(s) v(s) + i_0(s) \tag{24}$$

where diagonal terms of G are $(V_{\mathrm{in},k} + V_{F,k}) d_{w,k}(s)/h_k(s)$ and off-diagonal entries are zero.

Let us now prove that $G(s)$, $N(s)$ and $s\, i_0(s)$ converge to load-independent constant matrices $G^\star$, $N^\star$ and $i_0^\star$ when $s \to 0^+$, so that asymptotic expression of (24), i.e.

$$\begin{aligned} \lim_{t\to+\infty} i(t) &= \lim_{s\to 0^+} s(G(s) w/s - N(s) v(s) + i_0(s)) \\ &= G^\star w + i_0^\star - N^\star \lim_{s\to 0^+} s v(s) \\ &= G^\star w + i_0^\star - N^\star \lim_{t\to+\infty} v(t) \end{aligned} \tag{25}$$

[2] Note that $R_{D,k}$ appears to be a redundant parameter as d_k can be freely assigned via the parameter transfer functions $\tau_{i,k}$, $\tau_{\mathrm{ref},k}$ and $\tau_{v,k}$, whatever is $R_{D,k}$.

is nothing but (22). To this end, let $f_{w\mapsto i}(s)$ and $f_{w\mapsto v}(s)$ be the matrix transfer functions from w to i and v, respectively. Observe that

$$f_{w\mapsto v}(s) = p(s)\mathbf{1}_m^\intercal G(s) \quad (26)$$
$$f_{w\mapsto i}(s) = (\mathbf{I}_m - p(s)N(s)\mathbf{1}_m^\intercal)G(s) \quad (27)$$

where

$$p(s) := \frac{R + CRR_C s}{1 + C(R+R_C)s + \mathbf{1}_m^\intercal N(s)(R + CRR_C s)}$$

Indeed, (26) is derived by left multiplying (24) by $\mathbf{1}_m^\intercal$ and substituting the resulting expression of $\mathbf{1}_m^\intercal i = i_T$ into Laplace transform of (3b), which reads

$$(1 + C(R+R_C)s)v = (R + CRR_C s)\mathbf{1}_m^\intercal i, \quad (28)$$

so that

$$v = p(s)\mathbf{1}_m^\intercal(G(s)w + i_0/s) \quad (29)$$

holds. Then, the use of (24) and (29) gives (27) readily. Let us define $f^\star_{w\mapsto v}$, $f^\star_{w\mapsto i}$, $p^\star$ and $h_k^\star$ as the limits when $s \to 0^+$ of $f_{w\mapsto v}(s)$, $f_{w\mapsto i}(s)$, $p(s)$ and $h_k(s)$, respectively. We now use the facts that, for all $R > 0$, (i) $f^\star_{w\mapsto v}$ and $f^\star_{w\mapsto i}$ exist and have finite values since asymptotic stability is assumed and (ii) every entries of $f^\star_{w\mapsto v}$ is non-zero as location of the voltage equilibrium must depend on every w_k. By (26), fact (ii) implies that $p^\star \neq 0$ so that $\mathbf{1}_m^\intercal G^\star$ must be finite, by virtue of fact (i). Since $G(s)$ is diagonal, fact (ii) implies that $G^\star$ is finite. To prove that $N^\star$ is finite, it suffices to remark that $f^\star_{w\mapsto i} = G^\star - N^\star f^\star_{w\mapsto v}$ and to invoke fact (i). Finally, the fact that $i_0^\star$ is finite follows from asymptotic stability and (25).

It remains to prove that (23) holds. Suppose, by contradiction, that (23) is not satisfied, i.e. $\mathbf{1}_m^\intercal N^\star < 0$. Observe that $p^\star$ reads

$$p^\star = \frac{R}{1 + R\mathbf{1}_m^\intercal N^\star} \quad (30)$$

so that the load $R = -1/\mathbf{1}_m^\intercal N^\star > 0$ leads to infinite value of $p^\star$ which contradicts previous statement. This proves that (23) holds. □

Remark (Lemma VI.2 for (15)). As inner control law (15) verifies Assumption 2 and solves Step 1, Lemma VI.2 ensures that equilibrium induced by inner closed-loop (3) with (15) adopts the form (22). Indeed, by setting derivative of i_k to zero in (16), resulting equation takes the form (22) with $G = \mathrm{diag}\{\nu\}$, $N = \mathrm{diag}\{\beta'\}^{-1}\alpha'$ and $i_0 = \nu V_{\mathrm{ref}} - V_F$, every terms being load-independent. Also observe that inequality (23) trivially holds. ⌟

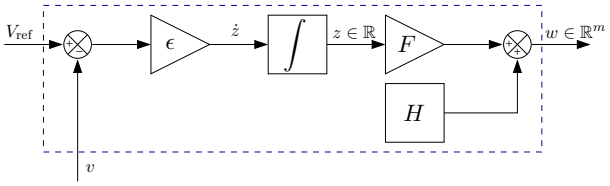

Fig. 6. Outer control law (32).

VII. Outer controller design

In this section, the outer controller $w(v)$ design which slowly drives the system toward $(i_{\mathrm{opt}}, V_{\mathrm{ref}})$ is discussed.

First observe that, together with (6), relationship (22) allows to write steady-state current and voltage as follows

$$i = (\mathbf{I}_m - \frac{N\mathbf{1}_m^\intercal}{1/R + \mathbf{1}_m^\intercal N})(Gw + i_0), \quad (31a)$$
$$v = \frac{\mathbf{1}_m^\intercal G w + \mathbf{1}_m^\intercal i_0}{1/R + \mathbf{1}_m^\intercal N}. \quad (31b)$$

The goal is to ensure that (i, v) equals $(i_{\mathrm{opt}}(R), V_{\mathrm{ref}})$ for all load. To this end, we might look for inner controller leading to G, N and i_0 in (22) for which there exists a constant vector w, to be determined, which guaranties that this optimal steady-state is always achieved. Finding solution of this problem (if any) might be intricate. Furthermore, some of the matrices G, N and i_0 will have to be load depend. Instead, we propose to let signal w be generated online via outer control layer described by

$$\dot{z} = \epsilon(V_{\mathrm{ref}} - v), \quad (32a)$$
$$w = Fz + H. \quad (32b)$$

and graphically represented Fig. 6.

By selecting $\epsilon > 0$ sufficiently small, dynamics of w can be made as slow as desired, which is equivalent to saying that ϵ is a tuning parameter for selecting relative aggressiveness of the inner loop w.r.t the outer loop. Thus, from the time-scale of w, closed-loop dynamics induced by inner controllers can be considered at the steady-state in accordance to the frequency separation principle, so that (22) and (31b) apply.[3] As shown by the following theorem, by assigning particular expression of F and H, it is possible not only to impose that v goes to V_{ref} but also to make i converge to i_{opt} for all R.

Theorem VII.1. *Given any inner controller verifying Assumption 2 and solving Step 1. Let G, N and*

[3] See e.g. [10] for standard results on systems with two time scales.

i_0 be defined as in Lemma VI.2. If F and H are given by

$$F = G^{-1}(\mathbf{1}_m - \Gamma\Psi r_1), \quad (33a)$$
$$H = G^{-1}\Gamma(\Psi r_1 \mathbf{1}_m^\intercal/m + (\Gamma^\intercal\Gamma)^{-1}\Gamma^\intercal)(V_{\text{ref}}N - i_0) - G^{-1}\Gamma\Psi r_2/2, \quad (33b)$$

then there exists $\epsilon_0 > 0$ such that for all $0 < \epsilon \leq \epsilon_0$ outer controller (32) solves Step 2.

Proof. Using (33) with (32b) gives

$$Gw = \mathbf{1}_m z + \Gamma J(z), \quad (34)$$

where

$$J(z) := -\Psi\left(r_1(z - \mathbf{1}_m^\intercal(V_{\text{ref}}N - i_0)/m) + r_2/2\right) + (\Gamma^\intercal\Gamma)^{-1}\Gamma^\intercal(V_{\text{ref}}N - i_0). \quad (35)$$

For ϵ sufficiently small, inner controller can be considered at the steady-state, so that (22) and (31b) apply. Hence, substituting v given by (31b) into (32a) and making use of (34) leads to

$$\dot{z} = \epsilon(V_{\text{ref}} - \frac{mz + \mathbf{1}_m^\intercal i_0}{1/R + \mathbf{1}_m^\intercal N}), \quad (36)$$

as $\mathbf{1}_m^\intercal\Gamma = \mathbf{0}$. By virtue of Lemma VI.2, inequality $\epsilon m/(1/R + \mathbf{1}_m^\intercal N) > 0$ holds for all $R > 0$ so that dynamics of z is stable. As a result, $\dot{z}^\star = 0$ which implies $v^\star = V_{\text{ref}}$ by (32a) and

$$z^\star = V_{\text{ref}}/(mR) + \mathbf{1}_m^\intercal(V_{\text{ref}}N - i_0)/m, \quad (37)$$

by (36). Using asymptotic value of v together with (34) allows to rewrite (22) as follows

$$i^\star = \mathbf{1}_m z^\star + \Gamma J(z^\star) - NV_{\text{ref}} + i_0.$$

Multiplying both side of this equality by the invertible matrix $[\mathbf{1}_m, \Gamma]^\intercal$ gives

$$\begin{bmatrix}\mathbf{1}_m^\intercal \\ \Gamma^\intercal\end{bmatrix} i^\star = \begin{bmatrix} mz^\star - \mathbf{1}_m^\intercal(V_{\text{ref}}N - i_0) \\ \Gamma^\intercal\Gamma J(z^\star) - \Gamma^\intercal(V_{\text{ref}}N - i_0)\end{bmatrix}.$$

as $\mathbf{1}_m^\intercal\Gamma = \mathbf{0}$. From (37) and (35), this expression reduces to

$$\begin{bmatrix}\mathbf{1}_m^\intercal \\ \Gamma^\intercal\end{bmatrix} i^\star = \begin{bmatrix} V_{\text{ref}}/R \\ -\Gamma^\intercal\Gamma\Psi(r_1\frac{V_{\text{ref}}}{mR} + \frac{r_2}{2})\end{bmatrix} = \begin{bmatrix}\mathbf{1}_m^\intercal \\ \Gamma^\intercal\end{bmatrix} i_{\text{opt}},$$

by recognizing the expression of $\Gamma^\intercal i_{\text{opt}}$ and $\mathbf{1}_m^\intercal i_{\text{opt}}$, deduced from (9). As a result, $i^\star$ equals i_{opt}. □

Observe that G, N and i_0 are load-independent for any inner controller verifying Assumption 2 and solving Step 1. In such a case, it is emphasized that, in contrast with $i_{\text{opt}}(R)$, matrices F and H does not depent on the unknown load R. In fact, the role played by the integrator (32a) is twofold: First, it regulates voltage v and, second, it estimates the value of R which can be deduced from $z^\star$ via (37). The knowledge of R is then used to assign optimal current sharing $i_{\text{opt}}(R)$ by inverting (31a).

Remark (Balanced current sharing). Balanced current sharing refers to the case where each $i_k^\star$ has the same value. Such a situation can be imposed by simply selecting F and H as follows

$$F = G^{-1}\mathbf{1}_m, \quad (38a)$$
$$H = G^{-1}\Gamma(\Gamma^\intercal\Gamma)^{-1}\Gamma^\intercal(V_{\text{ref}}N - i_0), \quad (38b)$$

while sticking to the same control scheme (32). This fact can be proven by means of similar developments to the proof of Th. VII.1: Matrix J, previously defined by (35), becomes $J = (\Gamma^\intercal\Gamma)^{-1}\Gamma^\intercal(V_{\text{ref}}N - i_0)$ so that $[\mathbf{1}_m, \Gamma]^\intercal i^\star = [V_{\text{ref}}/R, \mathbf{0}]^\intercal$ which is equivalent to $i^\star = \mathbf{1}_m V_{\text{ref}}/(mR)$ where each component shares the same value $V_{\text{ref}}/(mR)$. Note that such a steady-state coincides with the optimal one only when powerloss functions $p_k(i_k)$ are identical for every converter. Section VIII-B illustrates this point. ⌟

VIII. Experimental implementation

A. Experimental setup

The experimental setup, represented on Fig. 7, is composed of two buck converters ($m = 2$), which are heterogeneous in the sense that inductors as well as transistors are different ($L_1 = 1.3$mH and $L_2 = 0.6$mH, transistors 1 and 2 references are STP31510F7 and STP30NF10, respectively). It happens that electrical components of converter 2 have lower quality but its diode threshold voltage is lower. As a result, inequalities $r_{1,1} < r_{1,2}$ and $r_{2,1} > r_{2,2}$ hold and, in turn, induce inversion between converter having priority, depending on the load (see Section IV). This kind of configuration can appear when a fast synchronous buck converter with low power rating is used for converter 2 and a slower classical buck converter with higher power rating is used for converter 1.

Considering an input voltage $V_{\text{in},1} = V_{\text{in},2} = 24$V, (i) regulating voltage stability at the reference $V_{\text{ref}} = 12V$ and (ii) imposing optimal current i_{opt} through the two converters are control objectives to be achieved for any $R > 0$. The controller hardware is a dSpace MicroLabBox with switching frequency at 20kHz and sampling frequency at 10kHz.

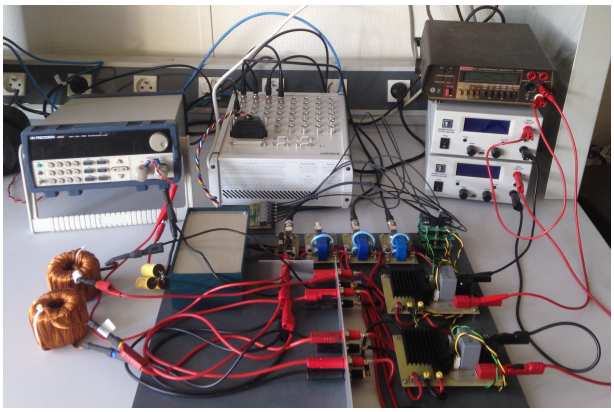

Fig. 7. Experimental setup.

R \ Solution	balanced (38)	optimal (33)
$R_1 = 12\Omega$	①	②
$R_2 = 1\Omega$	④	③

TABLE I
EXPERIMENTAL CONDITIONS.

B. Experimental results

Relying on inner control law (15), flexibility of the proposed control scheme is illustrated by comparing two outer controllers (32) that differ according to parameters F and H: Optimal solution (33) versus balanced solution (38). Along the experiments two different loads are used. Resulting four different cases are described by Table I and black crosses of Fig. 3 locates corresponding positions in the (i_1, i_2)-plan.

For initial conditions corresponding to steady-state of configuration ①, experiments are performed by switching from configurations ① to ④, successively. Results are represented by Fig. 8 which depicts currents through inductors (subplot 1), voltage v together with reference voltage V_{ref} (subplot 2) and duty cycles (subplot 3). Fig. 9 represents the currents in the (i_1, i_2)-plan. It shows that after short transient, for each configuration ① to ④ the crosses are correctly reached. During time interval ①, the desired voltage V_{ref} and uniform distribution $i_1 = i_2$ is maintained. For the same load, the control in ② achieves optimal losses by modifying current distribution and giving priority to converter 2. From ② to ③, the load variation shows that after a short transient, V_{ref} is reached and optimal distribution is achieved. Note that for this configuration i_2 is less than i_1 whereas the opposite was observed for ② (see Section IV). This behavior is consistent with Fig. 3 since ③ is located below the line $i_1 = i_2$ in contrast with ② which is above. For the last time interval ④, the currents are balanced, leading to higher losses as clearly shown by Fig. 3 since power level increases from ③ to ④.

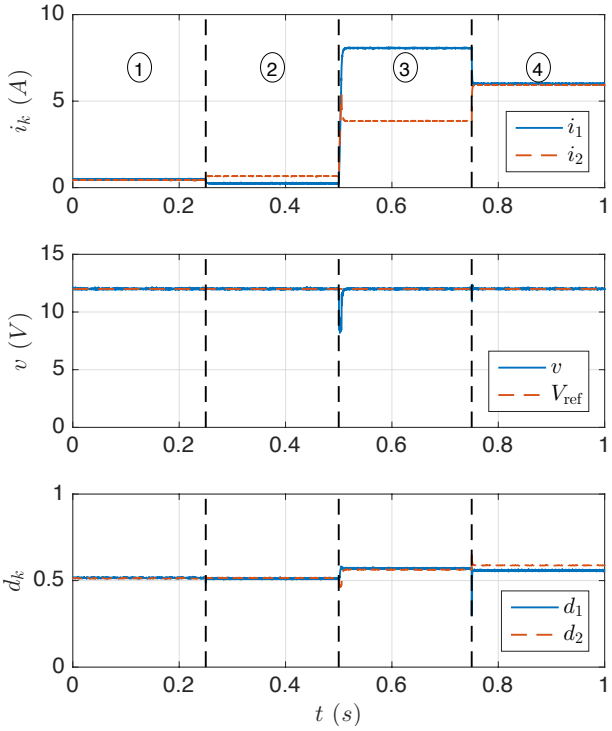

Fig. 8. Time experiments.

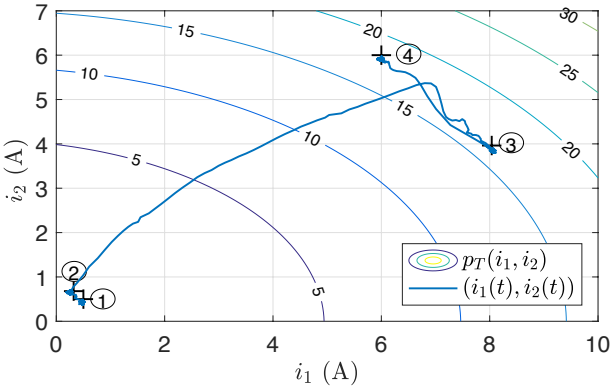

Fig. 9. Time experiments in the (i_1, i_2)-plan.

The efficiency of the optimal distribution compared with the balanced one is shown by measuring the losses in both cases. The losses are measured for different loads translated in terms of total current. Direct measurements of the input source power and

output dissipation power are performed to compute losses which are represented by Fig. 10. The upper subplot represents the measured total losses, for both optimal current i_{opt} and balanced current i_{bal}. The lower subplot represents downgrading with respect to the optimal power losses, defined by the ratio

$$\rho := (p_{\text{T}}(i_{\text{bal}}) - p_{\text{T}}(i_{\text{opt}}))/p_{\text{T}}(i_{\text{opt}}). \qquad (39)$$

Those pictures show that total losses are higher for the balanced strategy. The point where ratio $\rho = 0$ corresponds to the intersection of lines related to balanced and optimal currents on Fig. 3, for which optimal distribution is uniform.

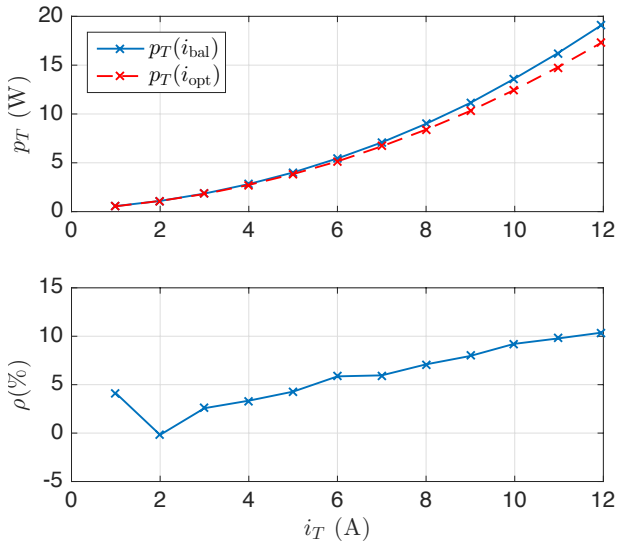

Fig. 10. Power losses (see (39) for the definition of ρ).

IX. Perspectives

Among many others, possible extensions of this work are the followings: (i) Consider discontinuous conduction mode, both in the dynamical equations and in the power losses expression, and (ii) gives the ability to the outer controller to select an optimal steady-state taking power limitations of each converters into account.

References

[1] V. J. Thottuvelil and G. C. Verghese, "Analysis and control design of paralleled dc/dc converters with current sharing," in *Applied Power Electronics Conference and Exposition, 1997. APEC'97 Conference Proceedings 1997., Twelfth Annual*, vol. 2. IEEE, 1997, pp. 638–646.

[2] Y. Huang and C. K. Tse, "Circuit theoretic classification of parallel connected dc-dc converters," *IEEE Transactions on Circuits and Systems I: Regular Papers*, vol. 54, no. 5, pp. 1099–1108, May 2007.

[3] A. Cid-Pastor, R. Giral, J. Calvente, V. Utkin, and L. Martinez-Salamero, "Interleaved converters based on sliding-mode control in a ring configuration," *IEEE Transactions on Circuits and Systems I: Regular Papers*, vol. 58, no. 10, pp. 2566–2577, Oct 2011.

[4] M. Hamzeh, A. Ghazanfari, Y.-R. Mohamed, and Y. Karimi, "Modeling and design of an oscillatory current-sharing control strategy in dc microgrids," *IEEE Transactions on Industrial Electronics*, vol. 62, no. 11, pp. 6647–6657, Nov 2015.

[5] M. Srinivasan and A. Kwasinski, "Autonomous hierarchical control of dc microgrids with constant-power loads," in *Applied Power Electronics Conference and Exposition (APEC), 2015 IEEE*, March 2015, pp. 2808–2815.

[6] J. Guerrero, J. Vasquez, J. Matas, L. de Vicuna, and M. Castilla, "Hierarchical control of droop-controlled ac and dc microgrids ; a general approach toward standardization," *IEEE Transactions on Industrial Electronics*, vol. 58, no. 1, pp. 158–172, Jan 2011.

[7] J.-F. Trégouët, R. Delpoux, and J.-Y. Gaulthier, "Optimal secondary control for dc microgrids," in *2016 IEEE 25th International Symposium on Industrial Electronics (ISIE)*, Santa Clara, CA, June 2016, pp. 510–515.

[8] M. K. Kazimierczuk, *Pulse-width modulated DC-DC power converters*. John Wiley & Sons, 2008.

[9] J.-Y. Gauthier, X. Lin-Shi, and A. Avramoae, "Predictive control with efficiency optimization and normalization for a multilevel converter," in *IEEE International Symposium on Sensorless Control for Electrical Drives*, oct 2013, pp. 1–6.

[10] H. K. Khalil, *Nonlinear Systems*, 2nd ed. Englewood Cliffs, NJ: Prentice-Hall, 1996.